IEEE Access
Multidisciplinary | Rapid Review | Open Access Journal

Received January 4, 2022, accepted January 28, 2022, date of publication February 1, 2022, date of current version February 9, 2022.

Digital Object Identifier 10.1109/ACCESS.2022.3148593

Empirical Implementation of the Steinmetz Equation to Compute Eddy Current Loss in Soft Magnetic Composite Components

MEHMET C. KULAN[1], NICK J. BAKER[1], KONSTANTINOS A. LIOGAS[2,3], OLIVER DAVIS[2], JOHN TAYLOR[2], AND ALEXANDER M. KORSUNSKY[3]

[1]School of Engineering, Merz Court, Newcastle University, Newcastle upon Tyne NE1 7RU, U.K.
[2]SG Technologies, Rainham RM13 9YH, U.K.
[3]Department of Engineering Science, University of Oxford, Oxford, Oxfordshire OX1 3PJ, U.K.

Corresponding author: Mehmet C. Kulan (mehmet.kulan@newcastle.ac.uk)

This work was supported in part by the Driving Electric Revolution (DER) Initiative through the U.K. Government under Innovate Grant 76019.

ABSTRACT Finite element analysis of magnetic materials allows accurate prediction of losses and is crucial in the design of electromagnetic devices and products. Soft magnetic composites are an alternative to silicon steel laminations, yet the electromagnetic material properties are less well documented and include uncertainties which can lead to inaccurate iron and Joule loss computations. The microstructure of soft magnetic composites, which is based on ferromagnetic particles coated by inorganic resistive insulation, makes the process of iron loss prediction unique. Composite core materials require further attention by design engineers in terms of the effect of component size and pressing processes on core loss predictions, which for laminations uses the well-known Steinmetz law. This study accesses the existing soft magnetic composite core loss modelling trends using experimentally measured results. The challenges of estimating and using Steinmetz core loss coefficients via curve fitting approaches are discussed. The study indicates that soft magnetic composite components need to be treated differently to laminated iron cores. Modelling the composite materials in finite element software requires experimentally informed loss models to be able to accurately compute power losses under varying magnetic flux density and electrical frequency. An approach is suggested which can predict iron losses to within 7%, but is only validated for component cross sectional areas of 144 mm^2 or less.

INDEX TERMS Core losses, eddy currents, electrical machines, iron loss, magnetic materials, magnetic testing, soft magnetic composite (SMC), Steinmetz equation.

I. INTRODUCTION

Recent efforts on the reduction of CO_2 emissions drive forward electrification and the ultimate goal is to achieve a more sustainable future. Highly efficient and sustainable electric propulsion and its sophisticated power electronic components depend on the use of magnetic materials to deliver optimal performance. Traditionally, the most common method for the manufacturing of electrical machines is laminating the magnetic cores to overcome the losses due to Faraday's magnetic induction [1]. Soft magnetic steels are the basis of laminated cores and with the recent developments in materials science and manufacturing, high performance laminated iron cores made from silicon-iron (SiFe), nickel-iron (NiFe) and cobalt-iron (CoFe) alloys remain the most common materials in electrical machines and similar magnetic devices such as transformers and inductors [1]. In the last two decades, Soft Magnetic Composites (SMCs) have attracted the attention of many researchers working on low frequency magnetic components with the applications in electrical machines [2], actuators [3], transformers etc. SMCs utilize iron powder metallurgy and are composed of high purity iron powders and surface coating for electrical insulation and mechanical bonding [4]–[6]. The iron particles have a diameter of about 100 μm with an insulation thickness less than 1 μm [6]. The coated iron powders are pressed into a solid magnetic core after several manufacturing steps including die pressing, heating and curing treatment [5] as illustrated in Fig. 1.

The associate editor coordinating the review of this manuscript and approving it for publication was Sonia F. Pinto.

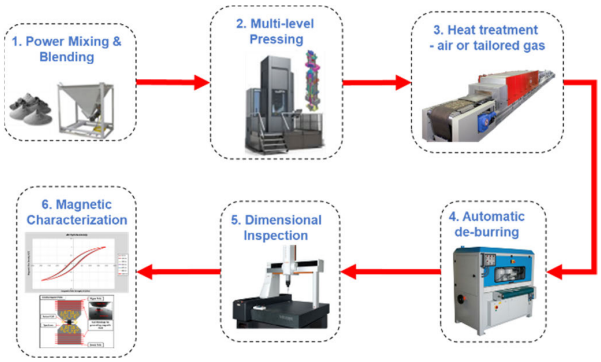

FIGURE 1. Parts production in soft magnetic composites: powder, compaction and heat treatment.

One of the key parameters in SMC is the powder to insulation ratio, affecting the resistivity of the composite. If the insulation is reduced in SMC, the electrical conductivity increases and thus the Joule (i.e. ohmic) losses will make it unfeasible for many applications such as motors and actuators where the efficiency is important.

A range of commercially available SMC powders are produced based on many parameters such as available powder grades, compaction regimes, heat treatments, secondary operations after compaction etc. These parameters usually lead to a trade-off between properties, for example:

- High magnetic permeability
- High electric insulation
- High mechanical strength

As depicted in Fig. 2 [7], it is not possible to highlight a unique SMC material giving the best mechanical strength and magnetic properties in parallel. Nevertheless, the isotropic nature of SMC opens up various three-dimensional (3D) magnetic design solutions.

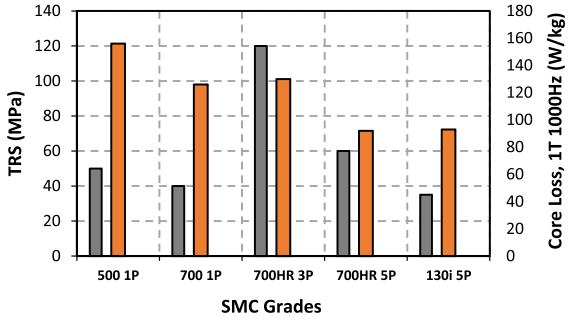

FIGURE 2. Somaloy (by Höganäs), Manufacturer supplied transverse rupture strength (TRS) and Core Losses (W/kg) of the 1P, 3P and 5P grades [7].

Early examples of electrical machines with SMC cores were investigated in [8]–[10]. Previous studies of SMC based electrical machines also dealt with power losses of SMC including hysteresis, particle eddy and bulk eddy current losses. Eddy current loss of the SMC is much lower than that of laminated electric steels due to the fact that SMC is composed of insulated iron powder particles. In the literature, many authors highlight this point for a potential application of SMC in electrical machines [1], [8], [9], [11]–[37].

Gao *et al.* investigated the SMC eddy current losses at particle level, stating that total eddy current losses can be represented by the sum of classical and anomalous eddy current losses [33]. This is an important finding to understand the eddy current characteristic of SMC but from the macroscopic point of view of modelling the SMC in FE software, it does not provide a concise approach.

Evangelista *et al.* utilized Box-Behnken design of experiments (DoE) approach to obtain Steinmetz coefficients of the commercially available Somaloy 3P 700 SMC [34]. For this investigation, they used 5 mm $\times$ 5mm ring samples produced under varying temperatures, compaction pressures and heat treatment duration. The results are valuable to understand the effect of technological parameters on the loss characteristic of the SMC. However, the proposed Steinmetz equation might not be used to model different geometries such as 3D flux machines, since the dependence of bulk eddy currents on the geometry was not considered to form the classical Steinmetz equation.

Wang *et al.* proposed a high performance axial flux PM machine with SMC cores for electric vehicles (EV) [38]. The machine benefits from toroidally wound internal stator and a 3D FE model has been used to investigate the performance. The core losses in SMC parts of S300b were computed by means of the manufacturer's W/kg data. Although this is the most straightforward approach in machine design, the provided W/kg data for SMCs cannot predict the losses accurately due to unaccounted geometry dependent cross-sectional areas within the SMC. This approach does not consider the variation of bulk eddy current losses.

Yu *et al.* studied harmonic effects on core loss in SMC materials [12]. They used frequency-domain Bertotti equations to predict the core losses when SMC is excited with sinusoidal and non-sinusoidal flux waveforms. This research is important as the magnetic flux density (B) in inverter driven PM machines will never be purely sinusoidal and additional B harmonics increase the core losses. Nevertheless, in their approach, they have not mentioned the dimensions of the sample ring which will prohibit the generalization of the acquired W/kg loss data for different geometries, shapes etc.

Liu *et al.* proposed a low cost transverse flux, flux switching PM machine with SMC cores [22]. They utilized ferrite and SMC cores to reduce the cost and investigated the performance of the proposed machine. As part of core loss analysis, they have done pre-experiments on SMC test rings of the same material, same density and the same heat treatment process as the SMC core used in the proposed machine's magnetic structure. Nonetheless, the core loss data acquired by the ring sample tests will never accurately predict the core losses within the active parts of the machine. This is because the ring sample tests mostly under estimate the bulk eddy current losses in SMCs, as it is a function of the component cross-sectional area.

Similarly, Kwon and Kim investigated the electromagnetic performance of a double-sided flat linear motor using SMCs [28]. The proposed machine uses Somaloy prototyping

material (SPM). In this study, iron and copper losses are investigated in terms of thermal limitation of the proposed machine. However, all iron loss results are dependent upon manufacturer provided W/kg core loss data which will be mostly inaccurate for different machine geometries.

On the other hand, the studies conducted by Potgieter *et al.* [18], [19] and Asama *et al.* [37] have more informative core loss calculation approaches. For instance, Asama *et al.* have used more than one toroidal test rings to measure the core losses of SMC [37]. The acquired data from the test rings were tabulated as W/kg loss data to compute SMC iron losses within FE software. Similarly, Potgieter *et al.* [18] acquire SMC loss data from test rings for machines operating up to 4 kHz and at flux density values of up to 2 Tesla. Their findings are very useful to characterize the electric machines operating at higher frequencies and deep saturation.

Electric machine designers mostly use pre-loaded material libraries in electromagnetic Finite Element (FE) simulations to compute the power losses via available W/kg loss data. This simple well established approach usually gives adequate prediction of losses in laminated machines, but in SMC based machines, this approach is often inaccurate. Nevertheless, some researchers acquire W/kg loss data with respect to varying peak magnetic flux density and frequency by conducting SMC ring sample tests in a closed loop system. Thus, they can set up a Steinmetz equation for SMC materials within the FE software.

Therefore, this paper aims to provide a more accurate loss calculation methodology for SMC based electrical machines and magnetic apparatus, but one that still uses commercial FE software. The paper is structured as follows. Firstly, core loss modelling and measurements in electrical machines via Steinmetz law and magnetic property testers are investigated respectively for SMC materials in order to highlight their capability for further loss estimations. Secondly, the challenges and potential errors in SMC loss modelling via very well-known classical Steinmetz equation are identified in FE software loss computations. Finally, the authors propose an experimentally informed FE loss modelling of SMC cores in order to enable more accurate predictions.

A. STEINMETZ EQUATION FOR SOFT MAGNETIC COMPOSITES

The weak insulation between the SMC particles causes additional eddy current loss that needs to be considered in different SMC geometries. In Fig. 3(a), the scanning electron microscopy (SEM) image of Somaloy 700 5P at 400 MPa is shown. The authors investigated the material microscopically and used rough image processing on an SEM image of Somaloy 700 5P to FE model the effect of bulk eddy currents on total losses.

Fig. 4 helps understand the effect of the mostly ignored bulk eddy current losses in SMC materials. The simulation considers alternating magnetic flux at 100 Hz. For the majority of machine designers, it is not feasible to model SMC at a

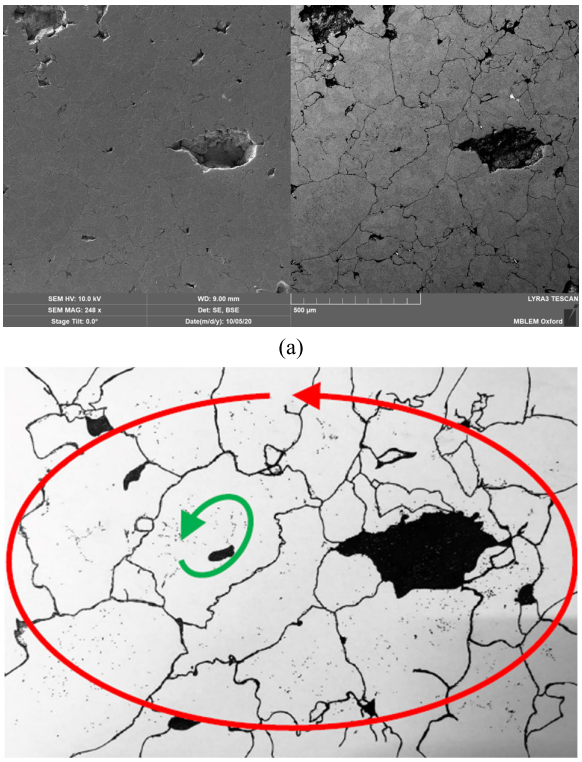

(a)

(b)

FIGURE 3. SMC images: (a) Somaloy 700 5P at 400 MPa, (b) green arrow: particle eddy current; red arrow: bulk eddy current causing additional losses.

microscopic level to obtain accurate loss analysis. In Fig. 4(a), eddy current loss in SMC is considered only at particle level. On the other hand, Fig. 4(b) demonstrates the worst case scenario when SMC particles have weak insulation and conducts the eddy currents in bulk material. It is calculated that eddy current losses in Fig. 4(b) is about 6.5-times higher than that illustrated in Fig. 4(a). This shows why SMC bulk eddy current losses might cause a significant mis-prediction of overall power losses.

The principal reason behind this is that the total power loss equation defined for SMC materials is of the form [39]:

$$P_{total} = K_h f^{\alpha} B^{\beta} + K_{ep} f^2 B^2 + \frac{B^2 f^2 d^2}{1.8 \times \rho \times resistivity \times 1000} (W/kg) \quad (1)$$

where K_h and K_{ep} are hysteresis and eddy current loss coefficients respectively; α and β are parameters to be determined from Steinmetz equation curve fitting; B and f are peak magnetic flux density (T) and electrical frequency (Hz) respectively and lastly d and ρ stands for the component's smallest cross-sectional dimension (mm) and mass density (g/cm^3), respectively. The unit of resistivity in (1) is $\mu\Omega$m. Hysteresis loss is due to change of magnetization and the eddy current loss occurs due to induced voltages in the electrically conducting material. In SMC, eddy current losses are lower than hysteresis losses but the effect of particle and bulk eddy current losses on the total loss becomes significant at

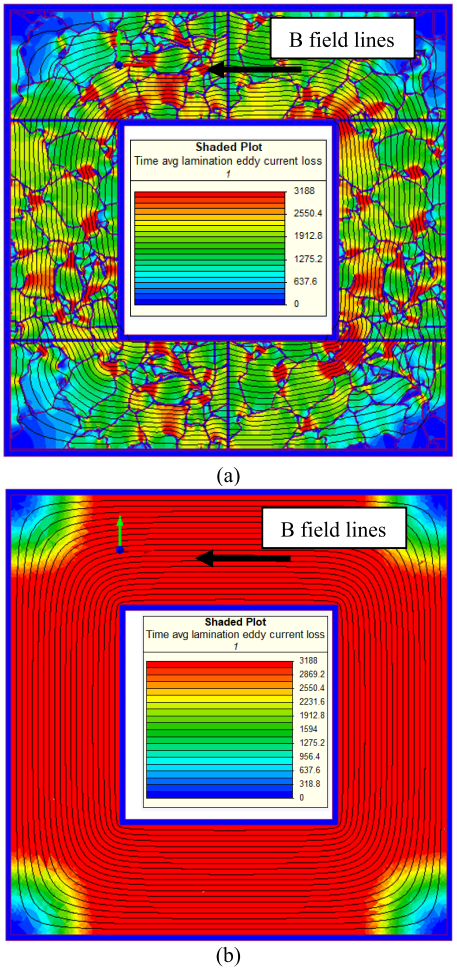

FIGURE 4. FEA modelling of SMC bulk eddy current losses, (a) Particle level SMC loss distribution, (b) Macroscopic level SMC loss distribution.

higher frequencies since eddy current loss is proportional to square of the frequency.

The authors in previous studies usually do not highlight the importance of eddy current loss in SMC and also they usually ignore the third term in equation (1) when W/kg loss data is converted to a classical Steinmetz equation by applying a curve fit. The well-known Steinmetz equation in commercial FE software to compute (usually post-processing) is given in (2):

$$P_{total} = K_h f^{\alpha} B^{\beta} + K_{ep} f^2 B^2 (W/kg) \tag{2}$$

The difference between (1) and (2) is the third term in (1) which stands for bulk eddy current loss. Bulk eddy current losses are dependent on the geometry and changes significantly with $'d'$. In addition, the accuracy of material resistivity is important to get the bulk eddy current loss in SMC correctly.

II. SMC TEST RINGS AND CORE LOSS MEASUREMENTS

A. TEST RING SAMPLES FOR MEASUREMENTS

In this study, a set of test rings given in Fig. 5(a) have been used to characterize the specific core losses and material resistivity. The main aim of the measurements is to compare the actual electromagnetic losses to those predicted through FE modelling. In laminated electrical machines, W/kg loss data acquired from conventional core loss tests (e.g. Epstein frame test) usually do not cause a problem in terms of accuracy of the loss data obtained. However, SMC differs from laminated electric steels and require more investigation before analyzing the core losses in FE software.

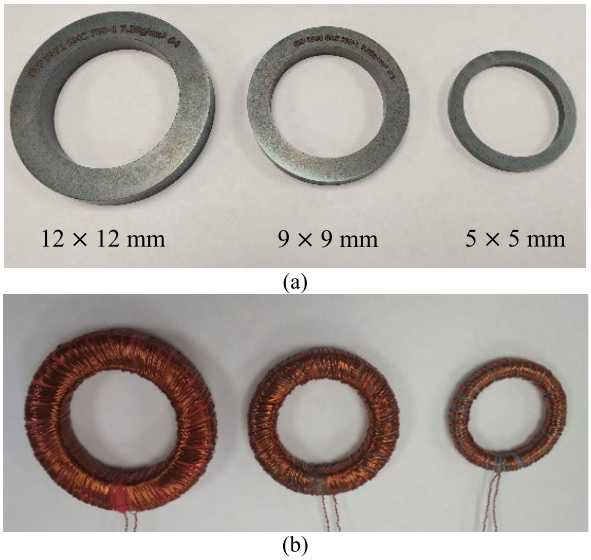

FIGURE 5. SMC components, (a) ring samples, (b) wound toroids.

To investigate the accuracy of iron loss prediction, focusing particularly on component size and the development of a practical and pragmatic way of using widely available Steinmetz law to predict losses in SMC, a set of iron rings has been fabricated with varying cross-sectional area. Fig. 5 (b) shows the largest and smallest of these rings, including a primary and secondary coil for applying magneto-motive force (MMF) and measuring electro-motive force (EMF) respectively. For each coil size, a number of alternative commercial grade SMC materials has been used to make a set of test rings which are believed to include the most likely grades, sizes, pressures and curing temperatures used for SMC components for real world motor designs. The SMC components are of Somaloy 700 1P by Höganas AB and pressed in different sizes and densities by SG Technologies, UK.

B. CORE LOSS MEASUREMENTS

There are several methods in existence to identify core losses in soft magnetic materials as explained in more detail by Fiorillo [40]. One of the most common methods is the two-winding watt-meter method. Toroid testers are the preferred method for material testing for SMC as mentioned in the relevant standards and as in [41]. Toroid tester method has therefore been used to determine core losses in SMC as illustrated in Fig. 6. In order to characterize SMC test ring samples two windings (primary N_1 and secondary N_2) are required where the primary winding is used to measure the magnetic flux density inside the core. The general schematic

of the test bench is shown in Fig. 7. The advantage of this characterisation setup is that only the test specimen with primary and secondary windings is magnetized. Therefore, there is no need to subtract additional effects of any magnetizing yokes or connect additional wirings to perform the measurements.

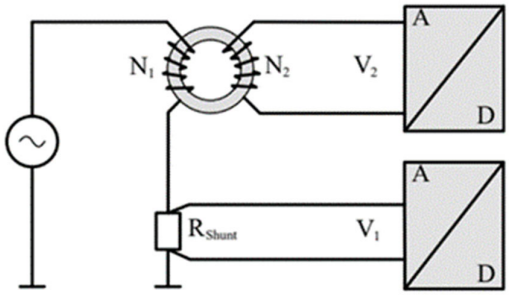

FIGURE 6. Schematic of toroidal tester.

The experimental setup consists of a Keysight 33522B function generator employed to generate the arbitrary waveform in different amplitudes and frequencies. The function generator output was connected to a 4-quadrant A1110-16-QE Hubert high precision amplifier that generated the magnetizing current on the ring. The output of the amplifier was connected to the primary winding N_1 of the specimen. For measuring the primary current, the built-in high precision resistance in the amplifier was used (R_{shunt}). To measure the flux density on the ring specimen, a secondary coil N_2 is utilised to extract the induced voltage. Because N_2 is connected a Keysight N2791A differential voltage probe with a high input impedance, the current in the secondary winding is negligible. Therefore, a thin wire was used. To ensure good coupling from primary to secondary, the secondary is wound under the primary coil [41]. Primary current and secondary induced voltage are converted from analogue to digital signals through a National Instrument PCI-6123 data acquisition card.

The advantage of this characterisation setup is that only the test speciment with a primary and secondary winding is magnetized. Iron losses of SMC test rings can be measured using the approach given below:

- Ring specimen path length l_e and cross-sectional area S need to be calculated (Equations (3) and (4) respectively).
- Weight and density of the specimen must be known.
- Magnetic field strength, H is calculated from a homogenous and air-gap free magnetic circuit by means of the Ampere's law (Eq. (5)).
- Magnetic flux density, B is calculated from the induced voltage on the secondary coil using Faraday's law (Eq. 6).

$$l_e = \frac{D_1 + D_2}{2}\pi(m) \tag{3}$$

$$S = \frac{D_1 - D_2}{2}h(m^2) \tag{4}$$

FIGURE 7. Iron loss measurement setup.

$$H = \frac{N_1 \cdot V_p}{l_e \cdot R_{Shunt}}(A/m) \tag{5}$$

$$B = -\frac{1}{N_2 S}\int V_s dt(T) \tag{6}$$

where,

N_1	=	Number of primary coil turns
N_2	=	Number of secondary coil turns
l_e	=	Path length, m
V_p	=	Primary coil voltage (V)
R_{Shunt}	=	Shunt electrical resistance (Ω)
S	=	Area of cross-section, (m^2)
V_s	=	Secondary coil voltage, (V)
f	=	Frequency (Hz)
T	=	Time period (sec)

In order to calculate the total iron loss in W/kg the material's density is included:

$$Core\ Loss = \frac{N_1 \cdot f}{N_2 \cdot S \cdot l_e \cdot R_{Shunt}}\int_0^T V_p \cdot V_s dt \tag{7}$$

By dividing (7) with the material density ρ in kg/m^3, the total iron loss in W/kg of the specimen can be derived. Primary current and secondary voltage are measured using the development system displayed in Fig. 6. With this setup, a closed loop control is possible. The closed loop control is necessary to calculate the parameters in the iron loss models, which must be determined under a controlled a sinusoidal flux density. As stated in [41] the form factor (FF) of flux density must be FF = 1.11 ± 1%. It has been observed that keeping this 1% limit at low flux densities is relatively easy, although it does get more challenging to keep the form factor within this band at the higher flux densities.

C. SMC RESISTIVITY TESTING

In contrast to laminated electric steels, SMC is a bulk material and its electrical resistivity is of importance in FE loss computations. Big SMC producers such as Höganas AB define the material resistivity for certain SMC grades and they use the four-point test method as depicted in Fig. 8. The resistivity value of the composite can be estimated if the cross-sectional area of the geometry, effective length between the measurement contacts and the resistance measured are known. The authors have observed that the density of the component

affects the measured resistivity values as the insulated particles of SMC deform more with the pressure, causing more electrically conductive paths.

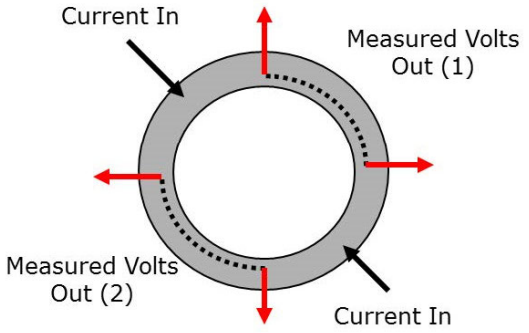

FIGURE 8. Four-point measurement setup for material resistivity.

The resistance measurements for Somaloy (by Höganas) S700 1P on 5 mm × 5 mm ring sample via four-point test method are given in Fig. 9. The validity of four-point test method is not yet proven across different SMC materials tested in this study.

The mis-prediction of component resistivity causes inaccurate bulk eddy current loss calculations and when the frequency increases in the presence of alternating magnetic field, the effect of wrong resistivity values will be more visible in the total power losses. Therefore, FE modelling of SMC based electromagnetic components is challenging and alternative methods have been considered where the electrical resistivity might be avoided to predict overall power losses in FE simulations.

III. MORE ACCURATE FINITE ELEMENT MODELLING OF SMC COMPONENTS

A. ELECTROMAGNETIC MODELLING OF TEST RINGS IN FEA

Toroid testers have been used experimentally for magnetic measurements as previously discussed in Section II, but SMC test ring samples can be modelled in different ways in a finite element software. Fig. 10 depicts a set of FE geometry that can be used as previously introduced in [42] to analyze the power loss and magnetic field distribution in SMC test ring samples.

Due to computational costs, 3D FE models are usually avoided if the 2D FE models are sufficiently accurate. All three FE models given in Fig. 10 have been simulated with an AC voltage source to compute the losses at particular magnetic flux density and frequency. It was noticed that the hysteresis losses can be computed equally accurate in all these models but eddy current losses can be captured better in 3D FE models due to the fact that eddy current paths, requiring z-axis are orthogonal to the direction of B, magnetic field on x-y plane. Magnetic flux lines are circumferential within the test ring samples.

Injecting pure AC current rather than AC voltage for the ring samples induces higher frequency magnetic field harmonics and it is not a correct approach to get the specific

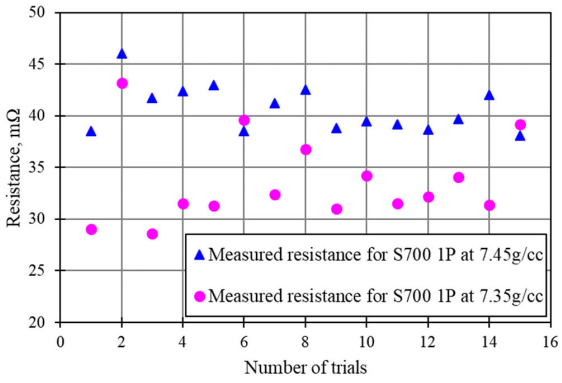

FIGURE 9. SMC 700-1P electrical resistance for a number of trials at different mass densities.

(W/kg) core losses as performed in the experiments. The closed loop magnetic test system does not allow any harmonics in B field and is purely sinusoidal. This is achieved with an alternating voltage source in FE simulations.

The accuracy of the loss results requires uniformity of the magnetic field within the cross-sections. Since the SMC components under investigation is toroid-like rings, the magnetic field inside a toroid can be calculated using the equation given in (8).

$$B = \frac{\mu_0 \mu_r N I}{2\pi r} \tag{8}$$

where μ_r is the relative permeability of the material, N is the number of turns, I is the current flowing in turns, and r is the average radius of the toroid from its center.

Peak voltage, V required to get a certain value of uniform magnetic field at a particular frequency, within the cross-sections of the ring samples, can be calculated by the (9). It is derived using a simple AC electrical circuit in phasors with a lumped resistance and inductance. Hence, a voltage source can be identified for different magnetic flux density values in varying frequencies.

$$|V| = \frac{2\pi r B}{\mu_0 \mu_r N} \left(\sqrt{\frac{\rho_c^2 l_c^2}{A_c^2} + \omega^2 \left(\frac{N^2 \mu_0 \mu_r A}{2\pi r}\right)^2} \right) \tag{9}$$

where B is peak magnetic flux density, N is number of turns, ρ_c is resistivity of the conductors, l_c is length of the conductors, A_c is the cross-sectional are of the conductor. A stands for the cross-sectional are of the ring sample and lastly ω is electrical angular frequency.

Modelling a toroid (i.e. test ring sample) with a voltage source in FE simulations causes transients due to inductance of the winding. The current achieves steady state after a certain time while it decays with an electrical time constant which is a function of coil inductance. For this reason, the 3D FE simulations have been solved until a steady state is reached. The acquired B field is purely sinusoidal in this case, as it is in the magnetic measurement experiments. For accurate FE loss results, a slice of 3D toroid (i.e. 2° mechanical) has been used as shown in Fig. 11 with field normal and flux

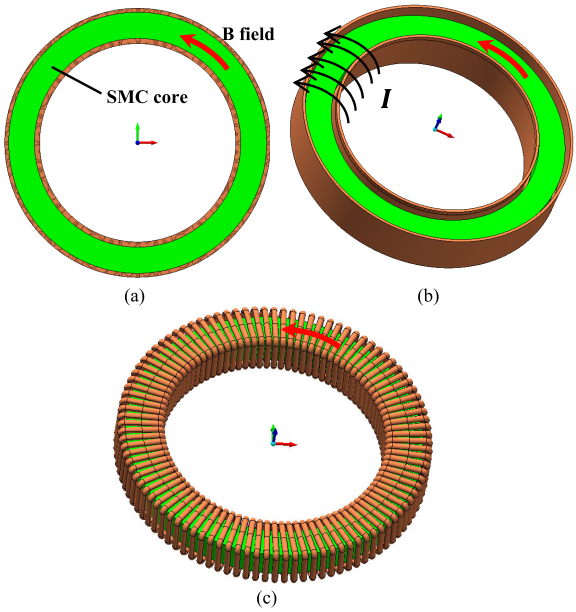

FIGURE 10. Finite element models of test ring samples (a) 2D FE model, (b) 3D FE model with copper foil wrapped around the ring sample, (c) 3D FE model of a toroidal sample (100 turns).

tangential magnetic boundary conditions (BC) to reduce the computational cost.

B. COMMON MISTAKES IN FE MODELLING OF SMC COMPONENTS USING MANUFACTURER'S W/KG LOSS DATA

Assuming that an SMC component will be modelled in an FE software and the manufacturer's W/kg loss data is known. The FE software generates a 2-term Steinmetz equation as given in (2) using the W/kg loss data entered. Also, the material electrical resistivity is known and added to the software to compute the Ohmic loss of the component. In this case, the user will end up with the following loss results from the FE simulations:

- Hysteresis loss due to change of magnetization under alternating current.
- Eddy current loss – usually called lamination eddy current losses in a commercial FE software.
- Ohmic or Joule losses due to material's bulk resistivity as depicted in Fig. 3(b).

In laminated magnetic components, Ohmic loss is not of interest as there is no bulk electrical resistivity of the component. However, in SMC based components, the bulk resistivity is of importance and the loss due to material conductivity needs to be added to the losses computed via Steinmetz equation defined in the software. Thus, overall power losses can be obtained. Nonetheless, this approach causes inaccurate loss modelling if the material is SMC. This is because the W/kg loss data of SMC does not work in the same way as it works in laminations. SMCs W/kg loss data includes Joule losses in addition to classical hysteresis and eddy current losses. Since it is not possible to segregate the geometry dependent Joule losses in the given W/kg loss data, the loss computations are

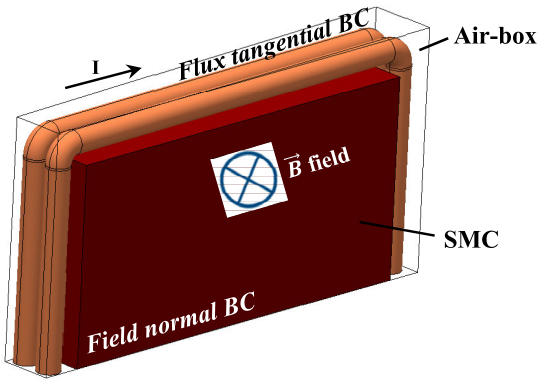

FIGURE 11. A slice (2°) of 3D toroid test ring sample with flux normal and tangential boundary conditions.

required to be done carefully in FE software if the material in this case, as explained in Fig. 12.

In Fig. 12, the W/kg core losses of Somaloy 700 1P were first obtained via magnetic measurements as described in Section II B. The same 5 mm × 5 mm SMC ring sample was later simulated to compare the loss results at 1 Tesla, 1 kHz. The overall W/kg losses are computed in two ways in the simulations:

- Classical hysteresis and eddy current losses are obtained via the FE simulations and Joule losses are later added analytically to get the overall losses.
- Classical hysteresis and eddy current losses are obtained via the FE simulations and also the FE software computed the Joule losses by using bulk material resistivity and $\vec{E}$ field ($\vec{J} = \sigma \vec{E}$). All loss components are added to get the total loss.

Both approaches given above inaccurately predict the original W/kg loss results calculated in the experiments as shown in Fig. 12. The error is up to 20%.

On the other hand, Fig. 13 compares the experimental and simulation results for the same material as given in Fig. 12. In this case, material resistivity and Joule loss computations are avoided in the software and the material W/kg loss data acquired by the experiments is used to get the Steinmetz equation coefficients via curve fitting. The loss results only consist of classical eddy and hysteresis losses. As given in Fig. 13, the FE results predict the total loss accurately, within an error of maximum 4.5%.

This states that the conversion of W/kg loss data from the experiments to the Steinmetz equation given in (2) and adding the Joule loss analytically or computationally to get the final losses will not lead to an accurate computation of total losses, because the experimental W/kg loss data includes not only classical eddy and hysteresis losses but also bulk eddy current (i.e. Joule) losses. Thus, mathematically some loss components are being double accounted due to the Steinmetz equation formed directly using the W/kg loss data. Therefore, machine designers need to be informed with a methodology to compute the losses in an FE software correctly. The bulk eddy current loss term (i.e. the third term in summation) given in equation (1) might cause a confusion for the machine

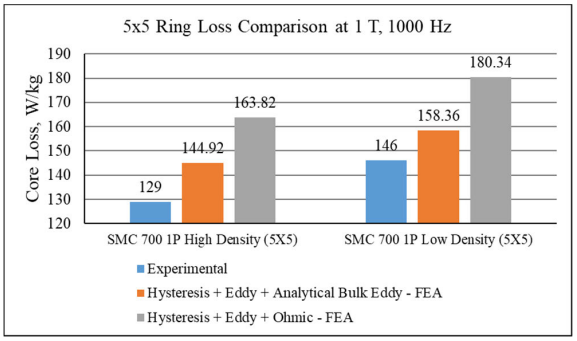

FIGURE 12. Experimental and finite element W/kg core loss comparisons for Somaloy 700 1P SMC test ring sample (5mm×5mm) at high and low densities.

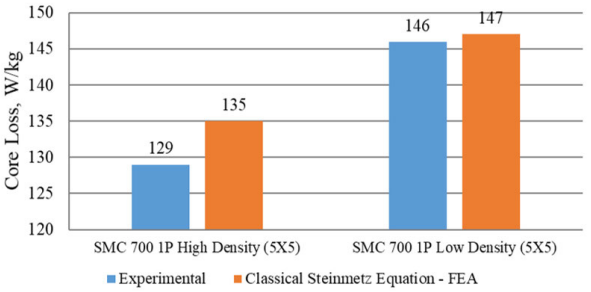

FIGURE 13. Experimental and finite element W/kg core loss comparisons for Somaloy 700 1P SMC test ring sample (5mm×5mm) at high and low densities and 1 T flux density. Only 2-term Steinmetz equation is used and bulk eddy current loss computation is avoided.

designers dealing with SMC electromagnetic modelling. This was addressed in Section IV.

IV. STEINMETZ EQUATION FOR SMC CORES

There are several accurate loss modelling options of SMC in FE simulations. Determining the Steinmetz coefficients (K_h and K_{ep}) via $[W/kg]$ loss data requires further attention and three approaches are discussed below.

A. OPTION 1 – THREE TERM MODIFIED STEINMETZ EQUATION FOR SMC

Two-term classical Steinmetz loss equation with K_h and K_{ep} (to be determined via curve-fitting) is revisited in equation (10).

$$P_{total} = K_h f^{\alpha} B^{\beta} + K_{ep} f^2 B^2 (W/kg) \tag{10}$$

However, for SMCs, equation (11) given below is the most accurate approach to model the losses of SMC in an FE software if the material resistivity and the geometrical coefficient, λ are both accurately known. The material density is denoted as ρ (g/cm^3).

$$P_{total} = K_h f^{\alpha} B^{\beta} + K_{ep} f^2 B^2 + \frac{B^2 f^2 d^2}{1.8 \times \rho \times \ resistivity \times 1000} (W/kg) \tag{11}$$

In classical textbooks, for thin laminations, the eddy current loss per unit volume is in the form [43], [44]:

$$p_e = \frac{\pi^2 B_m^2 f^2 t^2}{\lambda \times resistivity} (W/m \wedge 3) \tag{12}$$

where t is the lamination thickness (m), B_m is the peak magnetic flux density (T) and f stands for the frequency (Hz). λ is the geometrical coefficient and defined as [45], [46]:

$$\lambda = \frac{6}{1 - 0.633 \frac{w}{h} \tanh(1.58 \frac{h}{w})} \tag{13}$$

where w and h are width and height of the cross-sectional area and for $w \ll h$, equation (13) gives $\lambda = 6$, which is only true for thin laminations. Therefore, in equation (12), λ can be replaced by 6 if we consider laminations to calculate the eddy current losses analytically at certain frequencies. On the other hand, in equation (11), the third term which accounts for bulk eddy current losses is the same as given in (12). However, their units are not the same. If the equation (12) is converted into $[W/kg]$ form and is equated to the third term of (11), then:

$$p_e = \frac{B_m^2 f^2 t^2}{\rho \times resistivity} \times \frac{\pi^2}{\lambda} = \frac{B^2 f^2 d^2}{1.8 \times \rho \times resistivity \times 1000} \tag{14}$$

In (14), lamination thickness, t and the minimum cross-section length of SMC, d are the same parameters and 1000 in denominator stands for the unit conversion. Therefore, it can be written that:

$$\frac{\pi^2}{\lambda} = \frac{1}{1.8} \tag{15}$$

λ is found to be 17.765 if equation (11) is used to estimate the bulk eddy current losses for any SMC component, according to Höganas AB [47]. This is however not true for every geometry of SMC component. As an example, for a toroid with $w = h$ in (13), λ gives 14.3. This indicates that λ, the geometrical coefficient, is dependent upon the geometry and implies that the third term in (11) is required to be calculated analytically (i.e. post-processing) for the SMC components under loss investigation.

It should be also noted that equation (11) assumes that the material resistivity is accurately known. However, this is not the case for SMCs as explained in Section II C. (Fig. 9) For this reason, it is worth converting the three term Steinmetz equation given in (11) into a more classical Steinmetz equation as given in (10). Thus, inaccuracies due to material resistivity can be avoided in overall loss estimation of SMC components. The second and third term in (11) can easily be merged since particle and bulk eddy currents are both a function of $B^2 \times f^2$. The third term in (11) is however still important in terms of power loss *segregation* in SMCs, which is out of scope in this paper.

$$K_h f^{\alpha} B^{\beta} + \widetilde{K_{ep}} f^2 B^2 = K_h f^{\alpha} B^{\beta} + K_{ep} f^2 B^2 + \frac{B^2 f^2 d^2}{1.8 \times \rho \times resistivity \times 1000} \tag{16}$$

In equation (16), the updated eddy current loss coefficient is in the form:

$$\widetilde{K_{ep}} = K_{ep} + \frac{d^2}{1.8 \times \rho \times resistivity \times 1000} \tag{17}$$

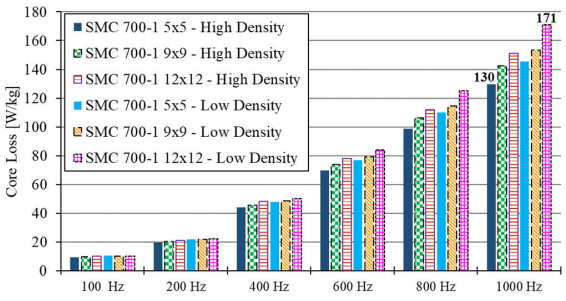

FIGURE 14. Measured Somaloy 700 1P core loss results with 1T sinusoidal flux density in W/kg for the test ring samples with the cross-sections of: 5mm×5mm, 9mm×9mm, 12mm×12mm.

If $\widetilde{K_{ep}}$ is used in curve-fitting as a parameter to be determined for the W/kg loss data at different frequencies and flux densities, the dimensional effects and the material resistivity are in fact substituted into an unknown of a two-term curve fitting with K_h and $\widetilde{K_{ep}}$ coefficients.

B. OPTION 2 – CLASSICAL STEINMETZ EQUATION (2-TERM CURVE FITTING)

The $[W/kg]$ loss data of SMC is forced to a curve fitting with classical Steinmetz loss equation as shown in (18).

$$P_{total} = K_h f^{\alpha} B^{\beta} + \widetilde{K_{ep}} f^2 B^2 (W/kg) \tag{18}$$

There is no distinction of eddy current losses as bulk and particle eddy current losses in this case. Therefore, two-term Steinmetz equation is sufficient to estimate the power losses without knowing the material resistivity. Joule losses due to the third term in (11) will be ignored within the FE software and the material resistivity should be taken as null in the FE simulations in this case.

In order to investigate losses of the ring samples given in Fig. 5 in FE simulations, equation (18) is adequate and it requires a curve fitting with parameters of K_h, $\widetilde{K_{ep}}$, α and β. The ring samples given in Fig. 5 are aimed to measure the specific loss of Somaloy 700 1P at different densities. The experimental loss information obtained by magnetic measurements of test ring samples will not be valid for other geometrical shapes such as complicated SMC segments designed for 3D flux machines as previously reported by the authors in [48]. This is due to the fact that bulk eddy currents, which are usually not considered as of importance in SMCs in the literature, vary with the component dimensions. This was clearly demonstrated in our experimental work. (Fig. 14)

In Fig. 14, the specific power loss of 12 mm × 12 mm ring sample is 41 W/kg higher than 5 mm × 5 mm ring sample at 1T and 1000 Hz. This is due to eddy currents circulating inside the ring samples. Specific power losses obtained via magnetic measurements such as Epstein frame tests for conventional laminations are assumed valid for all different stack lengths. These results prove there is no equivalent W/kg loss data valid for all different lengths of SMCs. Instead, SMC cores and cross-sectional dimensions which are orthogonal to the magnetic flux vector must be taken into account in bulk

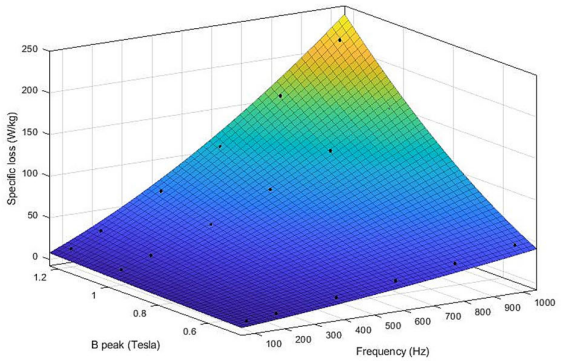

FIGURE 15. Curve-fitting for Loss=f (frequency, Bpeak) using three-term Steinmetz equation given in Eq.(11) for 9mm×9mm cross-section, Somaloy S700 1P at 7480 kg/m^3.

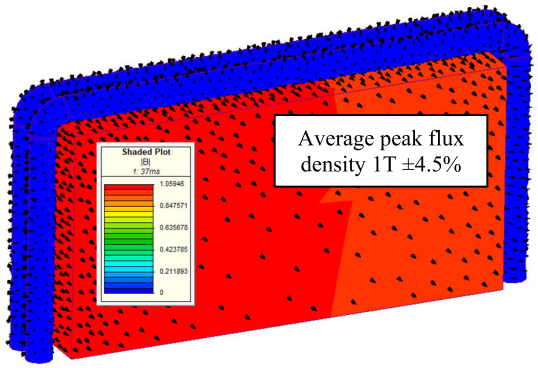

FIGURE 16. 3D FE simulation (2° slice) for S700 1P 9mm×9mm ring sample to compute specific power loss via classical 2-term Steinmetz equation.

eddy current loss computations. Therefore, 'Option 2' is an approach to find the power loss of the simple shapes like SMC toroids using FE software.

C. OPTION 3 - TWO-TERM AND THREE-TERM STEINMETZ EQUATIONS CURVE FITTING

In Section IV A&B, the Steinmetz equation has been explained for SMC. Curve fitting is the key to determine unknown parameters of a Steinmetz equation. Matlab® curve fitting tool was used to determine the coefficients and for the accuracy of the curve fitting, R-square and root mean square error (RMSE) values have been monitored. Levenberg-Marquardt and Trust-region algorithms are available in Matlab to apply the non-linear least squares method. In our case, the trust-region algorithm was implemented to fit a function with two variables: Loss $= f$(f, Bp) where f is frequency (Hz) and Bp is peak magnetic flux density (T).

In curve fitting, it was found that K_h remains almost constant with negligible variation but K_{ep} varies significantly with the different ring sizes. Fig. 15 depicts a curve-fitting with three-term Steinmetz equation for 9 mm × 9 mm ring sample with Somaloy 700 1P material at high density. Table 1 gives the goodness of fit for the model with 95% confidence bounds.

Similarly, two-term Steinmetz equation (see Eq. (10)) was also used to fit the W/kg loss data obtained at varying

TABLE 1. Three-term steinmetz equation curve fitting & goodness of fit for 9mm × 9mm S700 1P.

K_h with confidence bounds	0.0937 (0.06861, 0.1188)
K_{ep} with confidence bounds	2.796e-05 (1.99e-05, 3.603e-05)
a with confidence bounds	1.01 (0.9602, 1.06)
β with confidence bounds	1.683 (1.649, 1.717)
R-square	0.9999
RMSE	0.5622

TABLE 2. Two-term steinmetz equation curve fitting & goodness of fit for 9mm × 9mm S700 1P.

K_h with confidence bounds	0.0937 (0.06861, 0.1188)
K_{ep} with confidence bounds	5.412e-05 (4.605e-05, 6.218e-05)
a with confidence bounds	1.01 (0.9602, 1.06)
β with confidence bounds	1.683 (1.649, 1.717)
R-square	0.9999
RMSE	0.5622

frequencies and flux densities for the same ring sample. The curve-fitting summary table is given in Table 2.

It is clear from Table 1 and Table 2 that although K_h remains the same, eddy current coefficient K_{ep} increases in two-term Steinmetz equation since the third term (i.e. bulk eddy current term in eq. (11)) is transferred into the second term which is defined to be $\widetilde{K_{ep}}$ in equation (17). This approach is useful for FEA users as two-term Steinmetz equation is sufficient to model power loss and Joule loss calculations will not be needed and material will not be considered as electrically conductive, similar to laminations. This is, however, still a limited approach for SMCs since advanced modelling of SMCs might need post-processing with more than one Steinmetz equation defined for different sections of the whole geometry in order to get total loss very accurately. In Fig. 16, a 3D FE simulation is shown at 1T, 1 kHz for the ring sample and the power loss was computed by using the two-term Steinmetz equation where the coefficients were determined by curve fitting as shown in Fig 15.

V. EXPERIMENTALLY INFORMED SMC CORE LOSS MODELLING/ESTIMATION IN FEA

Experimental core loss tests are usually a prerequisite of SMC modelling in FE software to get a valid Steinmetz equation. From Section IV, it is understood that the geometry of SMC components is a parameter affecting the overall power loss. In the literature, some studies focus on SMC ring samples to acquire W/kg loss data which is later input to an FE software in order to simulate the losses in SMC based electrical machines [18], [37]. However, the dimensions of the ring samples chosen to measure the loss are arbitrary and the authors do not link the bulk eddy current loss to size of the ring under investigation. Traditionally, eddy current loss is not considered thoroughly in SMC since the particles of SMC are assumed to be insulated from each other.

Size of the ring is usually not an important parameter as long as the material is being magnetized at certain magnetic flux density and also the bulk eddy currents are not the case. However, in SMC, bulk eddy currents are significantly affected by the component's flux flowing window size where the $\vec{B}$ field is in normal direction.

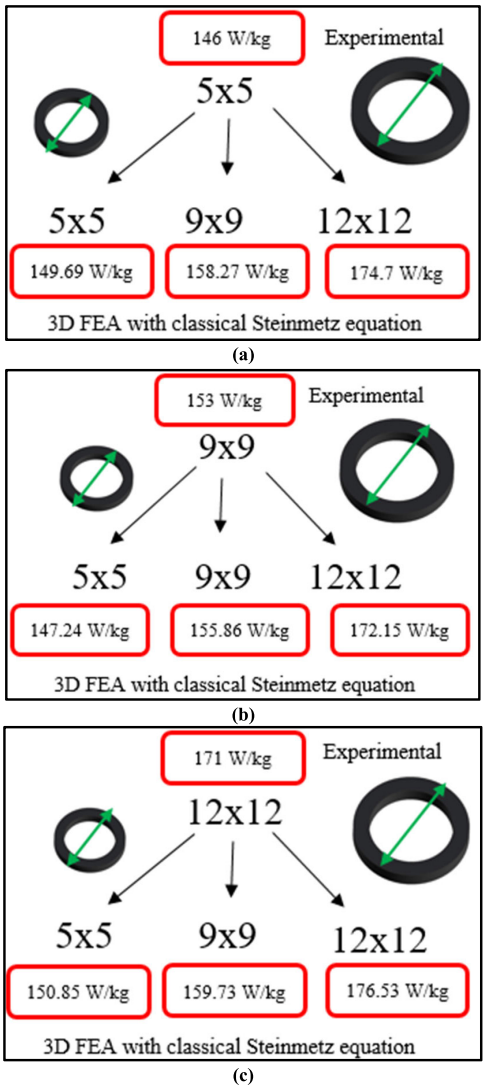

FIGURE 17. Specific (W/kg) power loss results for (a) 5mm×5mm, (b) 9mm×9mm and (c) 12mm×12mm ring samples: experimental vs 3D FE simulation results.

A. EXPERIMENTAL AND SIMULATION RESULTS

In Fig. 17, specific power losses of different sizes of ring samples are given. The SMC material used in experiments is Somaloy 700 1P. W/kg loss data obtained from 5 mm × 5 mm 5, 9 mm × 9 mm and 12 mm × 12 mm ring samples have been simulated among each other using equation (18) with the FE models of a toroid as exemplified in Fig.16. It is shown that the W/kg loss results are not the same for different rings sizes. For instance, if the loss data of 12 mm × 12 mm ring sample is used in simulations to get iron loss of 5 mm × 5 mm ring sample, it will be overestimated by 16%. Similarly, if the W/kg loss data of 5 mm × 5 mm ring is used in simulations to estimate the loss in 12 mm × 12 mm ring sample, then the total loss will be underestimated by 12.3%, confirming there

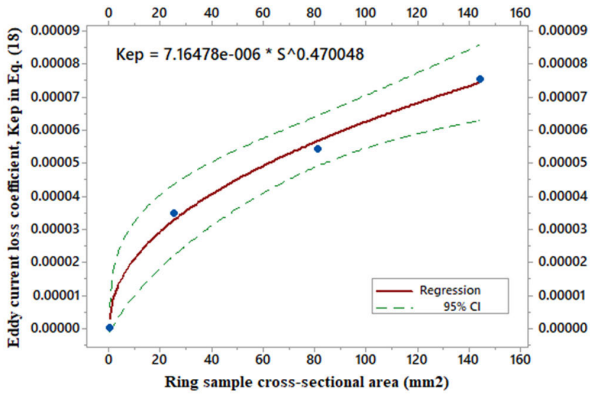

FIGURE 18. Non-linear regression analysis for the varying $\widetilde{K_{ep}}$ values in the experiments.

TABLE 3. Steinmetz equation coefficients given in (18) for different size of the ring samples – Somaloy 700 1P.

Ring size	K_h	$\widetilde{K_{ep}}$	α	β
5 mm × 5 mm	0.07683	3.47×10^{-5}	1.054	1.706
9 mm × 9 mm	0.0937	5.41×10^{-5}	1.01	1.683
12 mm × 12 mm	0.1021	7.51×10^{-5}	0.9901	1.707

is no unique set of W/kg loss data independent of component size.

Table 3 shows the coefficients of Steinmetz equation obtained for different sets of W/kg loss data from the ring samples: 5 mm × 5 mm, 9 mm × 9 mm and 12 mm × 12 mm. It is demonstrated that $\widetilde{K_{ep}}$ varies significantly for the experiments. This is due to the fact that inter-particle eddy currents circulate in the bulk material and contribute to overall eddy current loss. It should be noted that the greater the component size, the greater the inter-particle (i.e. bulk) eddy current losses since eddy currents formed in SMC components are geometry dependent as stated in equation (1). K_h is however changing slightly for different size of rings. Moreover, the exponential coefficients α and β are almost constant in two-term Steinmetz equations. The variation in $\widetilde{K_{ep}}$ needs to be considered to establish an equation working in a range of cross-sectional size of the ring samples. Thus, a more definitive Steinmetz equation can be written for a certain grade of SMC material to be used in low frequency electromagnetic FE simulations.

Since $\widetilde{K_{ep}}$ is a function of a ring's cross-section where $\vec{B}$ field is normal, mathematically $\widetilde{K_{ep}}$ can be written as a function of cross-sectional area by employing a non-linear regression as given below in Fig. 18.

In Fig. 18, a concave power function with two parameters is used. The equation was fitted via Gauss-Newton iterations and is in the form:

$$\widetilde{K_{ep}} = \theta_1 \times S^{\theta_2} \tag{19}$$

where θ_1 and θ_2 are parameters to be determined and S stands for the cross-sectional area where magnetic flux vector passes through. The parameters are estimated to be $\theta_1 = 7.164 \times 10^6$ and $\theta_2 = 0.470048$ as shown in Fig.18. If equation (19), which is a function of cross-sectional area, is substituted into equation (18), an empirical Steinmetz equation can be formed as given in (20).

TABLE 4. Application of equation (21) to a ring sample: 5 mm × 7mm – Somaloy 700 1P.

Component (Ring sample)	Specific power loss (Experimental)	Empirical Steinmetz in 3D FEA – Eq. (21)	Error (%)
5 mm × 7 mm	133 W/kg	141.01 W/kg	5.68

$$P_{total} = K_h f^{\alpha} B^{\beta} + \theta_1 \times S^{\theta_2} f^2 B^2 (W/kg) \tag{20}$$

where K_h, α, β, θ_1 and θ_2 are the parameters to be determined for varying cross-sectional area, S of the ring samples. Therefore, the proposed two-term Steinmetz equation will be more accurate as it is a function of the ring sample's size. However, equation (20) is constrained with the area, S and it is $S \in [0mm^2 - 144mm^2]$ since (19) was obtained for the ring samples up to 12 by 12. Furthermore, the ring samples larger than 12 by 12 have not been covered in this study, because it is difficult to test the larger ring samples at high magnetic flux densities under alternating current.

More specifically, Somaloy 700 1P was characterized and its Steinmetz equation $[W/kg]$ as a function of area, S is given in (21).

$$P = 0.0908 f^{1.018} B^{1.698} + 7.164 \times 10^{-6} S^{0.47} f^2 B^2 \quad S \in [0 - 144]\ in\ mm^2 \tag{21}$$

The accuracy of the proposed empirical Steinmetz equation was determined for a random ring size of 5 mm × 7 mm where the ring axial length is 7 mm. The results are given in Table 4.

The loss discrepancy for 5 mm × 7 mm ring sample is about 5.7% as given in Table 4. Assuming that the loss measurements are conducted on 9 mm × 9 mm ring to estimate the total loss in 5 mm × 7 mm ring, the computed FE loss will be 8% higher than the expected. The error rate will be even more if 12 by 12 ring sample is used.

The equations given in (20) and (21) are shown to be robust and will not allow the error to exceed ±7% for all ring samples with $S \in [0 - 144]$ in mm^2. This implies that the proposed empirical Steinmetz equation is a more general loss equation to estimate the SMC losses using an FE software and it reduces the risk of inaccurate loss modelling in SMC components due to dimensional variations and resistivity uncertainties. The proposed approach can be a part of experimentally informed finite element loss modelling of SMC cores. The whole process to compute core losses of SMC components more accurately through an electromagnetic FE software is summarized in a flowchart as given in Fig. 19.

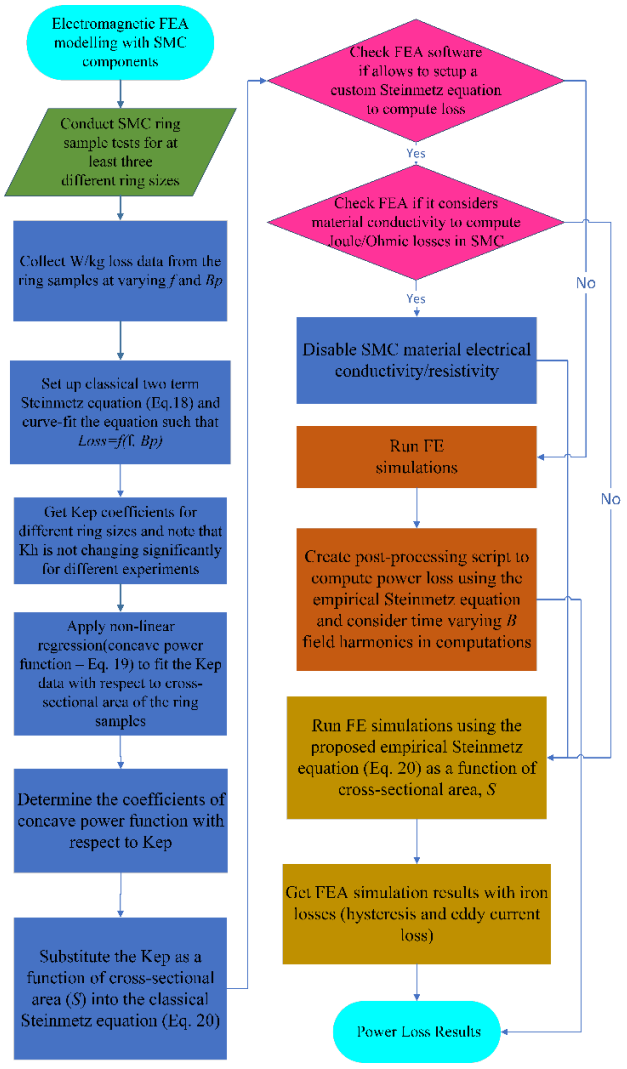

FIGURE 19. **Flowchart of the experimentally informed FE core loss computations via an empirical Steinmetz equation.**

VI. DISCUSSION

The authors provide a discussion to realize the challenges and methodology in SMC core loss modelling as follows:

- SMC resistivity acquired via four-point test method as discussed in Section II C gives a varying value and might cause significant error in overall loss.
- Three-term Steinmetz equation as given in equation (1) might be avoided in SMC core loss modelling if the material's resistivity is uncertain.
- Two-term Steinmetz equation as given in (18) is a better option to model core losses due to the fact that uncertainties in resistivity will not cause a significant core loss misprediction.
- Definition of $\widetilde{K_{ep}}$ given in (17) will help FE users to simplify the overall core loss computation in electromagnetic analysis and modelling.
- $\widetilde{K_{ep}}$ is calculated empirically from the experimental data by varying the size of ring samples and this is a more robust approach to include the bulk eddy current loss variations within an SMC component.
- Hysteresis loss coefficient, K_h in Steinmetz equation is usually a constant for a certain material/SMC grade. However, the authors experience that K_h slightly differs when the ring size changes. This is however an artificial error due to a non-linear curve-fitting and it is related with a lack of fit due to a limited number of experimental W/kg loss data. For more precision, the loss data points in varying magnetic flux density and frequency might be increased.
- The accuracy of proposed empirical Steinmetz equations given in (20) and (21) are dependent upon the accuracy of curve-fitting and it is constrained with the sizes of the rings used in the experiments.
- FE software users could ideally define more than one Steinmetz equation for different sections of the geometry to accurately compute the overall power loss. This is because W/kg loss data coming from the magnetic measurements are sensitive to the size of ring samples. Therefore, the authors propose an alternative Steinmetz equation benefiting from an expression as a function of cross-sectional area where magnetic flux passes through.
- Post processing is of importance for SMC loss computations as there will not be a unique Steinmetz equation for different geometries. Therefore, the FE users might consider divide the geometry into smaller sections to apply a number of Steinmetz equations via post processing in some software such as Matlab® or Excel. This however requires experimental magnetic pre-measurements to characterize the loss in different SMC components.
- It should be noted that SMC loss modelling is still challenging and requires many magnetic measurements to characterize the W/kg losses.
- The acquisition of eddy current loss parameters of SMCs might be affected by different working environments, compaction regimes and heat treatments. Therefore, it is important to highlight that the highest available accuracy can be achieved by using the same pressing tool under similar ambient conditions and heat treatment approach.

VII. CONCLUSION

The approach followed by most electrical machine designers to compute the power losses in any topology is to use finite element analysis. Where available, core loss computations rely on manufacturer's W/kg loss data. This approach has been shown to be of limited accuracy for SMC components as several uncertainties need to be considered.

In this paper, three approaches to using experimentally measured data as the input to finite element loss data were investigated. Dimensional factor and material resistivity in SMC are shown to be the main sources of error in loss computations. The paper proposes an empirical approach to estimate the eddy current loss in SMC to within $\pm 7\%$ using a two term robust Steinmetz equation, independent of material resistivity but only valid for a specific cross section of component up to 144 mm^2. It predicts total loss iron, but is not suitable for

loss segregation between hysteresis, bulk and particle eddy components of iron loss.

ACKNOWLEDGMENT

The authors acknowledge engineers and technicians in SG Technologies, Rainham, U.K., for their contribution to the manufacture winding and magnetic tests of SMC ring samples.

REFERENCES

[1] A. Krings, A. Boglietti, A. Cavagnino, and S. Sprague, "Soft magnetic material status and trends in electric machines," *IEEE Trans. Ind. Electron.*, vol. 64, no. 3, pp. 2405–2414, Mar. 2017.
[2] N. J. Baker and S. Jordan, "Comparison of two transverse flux machines for an aerospace application," *IEEE Trans. Ind. Appl.*, vol. 54, no. 6, pp. 5783–5790, Jun. 2018.
[3] M. Raihan, N. Baker, K. Smith, and A. Almoraya, "Development and testing of a novel cylindrical permanent magnet linear generator," *IEEE Trans. Ind. Appl.*, vol. 56, no. 4, pp. 3668–3678, Jul./Aug. 2020.
[4] Y. G. Guo, J. G. Zhu, P. A. Watterson, and W. Wu, "Development of a PM transverse flux motor with soft magnetic composite core," *IEEE Trans. Energy Convers.*, vol. 21, no. 2, pp. 426–434, Jun. 2006.
[5] L.-O. Pennander, "Recent development of soft magnetic composite materials and its application," in *Proc. Int. Symp. Magn. Bearings (ISMB)*, 2014, pp. 1–4.
[6] *Powder Metallurgy Meets Electromagnetics*. Accessed: Oct. 17, 2021. [Online]. Available: https://www.gknpm.com/globalassets/downloads/powder-metallurgy/2018/electromagnetic-application_brochure.pdf/
[7] *Soft Magnetic Composite (SMC) Somaloy Technology*. Accessed: Oct. 17, 2021. [Online]. Available: http://www.hoganas.com/en/business-areas/electric-drive-systems/motor-technology/somaloy-technology/
[8] A. G. Jack, "Experience with the use of soft magnetic composites in electrical machines," in *Proc. Int. Conf. Electr. Mach.*, İstanbul, Turkey, 1998.
[9] T. J. Hammons, H. B. Ertan, J. A. Tegopoulos, W. Drury, M. Ehsani, T. Nakata, and A. G. Jack, "Highlights of the 1998 international conference on electrical machines," in *Proc. ICEM Rev.*, 1998.
[10] A. G. Jack *et al.*, "Permanent magnet machines with powdered iron cores and pre-pressed windings," in *Proc. Conf. Rec. IEEE Ind. Appl. Conf. 34th IAS Annu. Meeting*, vol. 1, Oct. 1999, pp. 97–103.
[11] J. G. Zhu, Y. G. Guo, Z. W. Lin, Y. J. Li, and Y. K. Huang, "Development of PM transverse flux motors with soft magnetic composite cores," *IEEE Trans. Magn.*, vol. 47, no. 10, pp. 4376–4383, Oct. 2011.
[12] X. Yu, Y. Li, Q. Yang, C. Zhang, Y. Liu, and X. Gong, "Research of harmonic effects on core loss in soft magnetic composite materials," *IEEE Trans. Magn.*, vol. 55, no. 2, pp. 1–5, Feb. 2019.
[13] W. J. Xu, N. Duan, S. Wang, Y. Guo, and J. Zhu, "Modeling and measurement of magnetic hysteresis of soft magnetic composite materials under different magnetizations," *IEEE Trans. Ind. Electron.*, vol. 64, no. 3, pp. 2459–2467, Mar. 2017.
[14] S. Sun, F. Jiang, T. Li, B. Xu, and K. Yang, "Comparison of a multi-stage axial flux permanent magnet machine with different stator core materials," *IEEE Trans. Appl. Supercond.*, vol. 30, no. 4, pp. 1–6, Jun. 2020.
[15] A. Schoppa, P. Delarbre, E. Holzmann, and M. Sigl, "Magnetic properties of soft magnetic powder composites at higher frequencies in comparison with electrical steels," in *Proc. 3rd Int. Electr. Drives Prod. Conf. (EDPC)*, Oct. 2013, pp. 1–5.
[16] A. Schoppa and P. Delarbre, "Soft magnetic powder composites and potential applications in modern electric machines and devices," *IEEE Trans. Magn.*, vol. 50, no. 4, pp. 1–4, Apr. 2014.
[17] J. H. J. Potgieter, F. J. Márquez-Fernández, A. G. Fraser, and M. D. McCulloch, "Performance evaluation of a high speed segmented rotor axial flux switched reluctance traction motor," in *Proc. XXII Int. Conf. Electr. Mach. (ICEM)*, Sep. 2016, pp. 531–537.
[18] J. H. J. Potgieter, F. J. Márquez-Fernández, A. G. Fraser, and M. D. McCulloch, "Effects observed in the characterization of soft magnetic composite for high frequency, high flux density applications," *IEEE Trans. Ind. Electron.*, vol. 64, no. 3, pp. 2486–2493, Mar. 2017.
[19] J. H. Potgieter, F. J. Márquez-Fernández, A. Fraser, and M. D. McCulloch, "Loss coefficient characterisation for high frequency, high flux density, electrical machine applications," in *Proc. IEEE Int. Electr. Mach. Drives Conf. (IEMDC)*, May 2015, pp. 1265–1271.
[20] A. Maruo and H. Igarashi, "Analysis of magnetic properties of soft magnetic composite using discrete element method," *IEEE Trans. Magn.*, vol. 55, no. 6, pp. 1–5, Jun. 2019.
[21] C. Liu, G. Lei, T. Wang, Y. Guo, Y. Wang, and J. Zhu, "Comparative study of small electrical machines with soft magnetic composite cores," *IEEE Trans. Ind. Electron.*, vol. 64, no. 2, pp. 1049–1060, Feb. 2017.
[22] C. Liu, G. Lei, B. Ma, Y. Wang, Y. Guo, and J. Zhu, "Development of a new low-cost 3-D flux transverse flux FSPMM with soft magnetic composite cores and ferrite magnets," *IEEE Trans. Magn.*, vol. 53, no. 11, pp. 1–5, Nov. 2017.
[23] Y. L. Lim, N. Ertugrul, and W. L. Soong, "Methods and verification of loss breakdown in an AC brushless PM soft magnetic composite machine," in *Proc. IEEE 12th Int. Conf. Power Electron. Drive Syst. (PEDS)*, Dec. 2017, pp. 761–768.
[24] G. S. Liew, N. Ertugrul, W. L. Soong, and D. B. Gehlert, "Analysis and performance evaluation of an axial-field brushless PM machine utilising soft magnetic composites," in *Proc. IEEE Int. Electr. Mach. Drives Conf.*, May 2007, pp. 153–158.
[25] G. S. Liew, E. C. Y. Tsang, N. Ertugrul, W. L. Soong, D. Atkinson, and D. B. Gehlert, "Analysis of a segmented brushless PM machine utilising soft magnetic composites," in *Proc. 33rd Annu. Conf. IEEE Ind. Electron. Soc. (IECON)*, 2007, pp. 1268–1273.
[26] Y. Li, Q. Yang, J. Zhu, and Y. Guo, "Magnetic properties measurement of soft magnetic composite materials over wide range of excitation frequency," *IEEE Trans. Ind. Appl.*, vol. 48, no. 1, pp. 88–97, Jan./Feb. 2012.
[27] Y. Li, Y. Liu, F. Liu, Q. Yang, and P. Ren, "Magnetic anisotropic properties measurement and analysis of the soft magnetic composite materials," *IEEE Trans. Appl. Supercond.*, vol. 24, no. 5, pp. 1–4, Oct. 2014.
[28] Y.-S. Kwon and W.-J. Kim, "Electromagnetic analysis and steady-state performance of double-sided flat linear motor using soft magnetic composite," *IEEE Trans. Ind. Electron.*, vol. 64, no. 3, pp. 2178–2187, Mar. 2017.
[29] Y. G. Guo and J. G. Zhu, "Applications of soft magnetic composite materials in electrical machines: A review," *Austral. J. Electr. Electron. Eng.*, vol. 3, no. 1, pp. 37–46, 2006.
[30] Y. Guo, J. G. Zhu, P. A. Watterson, and W. Wu, "Comparative study of 3-D flux electrical machines with soft magnetic composite cores," *IEEE Trans. Ind. Appl.*, vol. 39, no. 6, pp. 1696–1703, Nov. 2003.
[31] Y. Guo, J. Zhu, H. Lu, Z. Lin, and Y. Li, "Core loss calculation for soft magnetic composite electrical machines," *IEEE Trans. Magn.*, vol. 48, no. 11, pp. 3112–3115, Nov. 2012.
[32] Y. Gao, T. Fujiki, H. Dozono, K. Muramatsu, W. Guan, J. Yuan, C. Tian, and B. Chen, "Modeling of magnetic characteristics of soft magnetic composite using magnetic field analysis," *IEEE Trans. Magn.*, vol. 54, no. 3, pp. 1–4, Mar. 2018.
[33] Y. Gao, Y. Araki, H. Dozono, K. Muramatsu, W. Guan, J. Yuan, C. Tian, and B. Chen, "Modeling of anomalous eddy current losses due to movement of domain walls in particles of a soft magnetic composite," *IEEE Trans. Magn.*, vol. 56, no. 4, pp. 1–4, Apr. 2020.
[34] L. Evangelista, M. A. Carvalho, and P. A. P. Wendhausen, "Steinmetz coefficients' prediction based on processing parameters of soft magnetic composites," *IEEE Trans. Magn.*, vol. 56, no. 2, pp. 1–5, Feb. 2020.
[35] G. Cvetkovski and L. Petkovska, "Performance improvement of PM synchronous motor by using soft magnetic composite material," *IEEE Trans. Magn.*, vol. 44, no. 11, pp. 3812–3815, Nov. 2008.
[36] J. Cros, P. Viarouge, and M. T. Kakhki, "Design and optimization of soft magnetic composite machines with finite element methods," *IEEE Trans. Magn.*, vol. 47, no. 10, pp. 4384–4390, Oct. 2011.
[37] J. Asama, T. Oiwa, T. Shinshi, and A. Chiba, "Experimental evaluation for core loss reduction of a consequent-pole bearingless disk motor using soft magnetic composites," *IEEE Trans. Energy Convers.*, vol. 33, no. 1, pp. 324–332, Mar. 2018.
[38] Y. Wang, J. Lu, C. Liu, G. Lei, Y. Guo, and J. Zhu, "Development of a high-performance axial flux PM machine with SMC cores for electric vehicle application," *IEEE Trans. Magn.*, vol. 55, no. 7, pp. 1–4, Jul. 2019.
[39] Z. Ye, "Modelling and experimental analysis of core losses of SMC components," in *Proc. World Congr. Powder Metall. Particulate Mater. (PM)*, 2014, pp. 1–9.
[40] F. Fiorillo, *Characterization and Measurement of Magnetic Materials*. New York, NY, USA: Academic, 2004.
[41] *Methods of Measurement of the Magnetic Properties of Magnetically Soft Metallic and Powder Materials at Frequencies in the Range 20 Hz to 200 kHz by the Use of Ring Specimens*, Standard IEC 60404-6:2003, 2003.

[42] A. E. D. S. Bento, "Toroid inductor development for a SIC DC-DC converter up to 150 kW, based on finite element method," Ph.D. dissertation, Inst. Superior Engenharia Lisboa, Lisbon, Portugal, 2015.
[43] J. Edwards, *Electrical Machines and Drives*. New York, NY, USA: Macmillan, 1991.
[44] T. A. Lipo, *Introduction to AC Machine Design*. Hoboken, NJ, USA: Wiley, 2017.
[45] T. D. Shen, U. Harms, and R. B. Schwarz, "Bulk Fe-based metallic glass with extremely soft ferromagnetic properties," *Mater. Sci. Forum*, vols. 386–388, pp. 441–446, Jan. 2002.
[46] R. Sikora, J. Purczynski, W. Lipinski, and M. Gramz, "Use of variational methods to the eddy currents calculation in thin conducting plates," *IEEE Trans. Magn.*, vol. MAG-14, no. 5, pp. 383–385, Sep. 1978.
[47] *Somaloy Material Data*. Accessed: Nov. 9, 2021. [Online]. Available: https://www.hoganas.com/globalassets/download-media/sharepoint/brochures-and-datasheets—all-documents/somaloy-5p_material-data_june_2018_2274hog.pdf
[48] M. C. Kulan, N. J. Baker, and S. Turvey, "Manufacturing challenges of a modular transverse flux alternator for aerospace," *Energies*, vol. 13, no. 16, p. 4275, Aug. 2020.

MEHMET C. KULAN received the B.Sc. degree in electrical and electronics engineering from Bilkent University, Ankara, Turkey, in 2011, and the M.Sc. and Ph.D. degrees from the University of Newcastle Upon Tyne, U.K., in 2013 and 2018, respectively, as part of the Electrical Power Research Group, School of Engineering. His research interests include electromagnetics, thermal management of electrical machines, and finite element modeling of electric motors and alternators. He is currently working on core loss modeling in electrical machines and active magnetic bearings at the Electrical Power Research Group, Newcastle University.

NICK J. BAKER received the M.Eng. degree in mechanical engineering from Birmingham University, Birmingham, U.K., in 1999, and the Ph.D. degree in electrical machine design for marine renewable energy devices from Durham University, Durham, U.K., in 2003. He was a Researcher of machine design at Durham University in addition to academic posts within the Lancaster University's Renewable Energy Group, from 2005 to 2008, and currently with the Newcastle University's Electrical Power Group. He has spent a period in industry as a Senior Consultant for energy consultancy TNEI Services, Ltd., Newcastle, U.K., from 2008 to 2010. He is a Senior Lecturer and working on machines across the renewable, automotive, and aerospace sectors.

KONSTANTINOS A. LIOGAS received the B.Eng. degree (Hons.) in electrical and electronic engineering from the University of East London, U.K., in 2017. He is currently pursuing the Doctor of Philosophy (D.Phil.) degree in engineering sciences with the St. Catherine's College, University of Oxford. In parallel with his studies, he worked as a Research Engineer at SG Technologies Ltd., Rainham, U.K. At SG Technologies, he has been heavily involved in the research and development of novel soft and hard magnetic materials for high-efficiency electrical machines and other electromagnetic devices. He is a member of Prof. Korsunsky's research group. His research interests include quantifying the relationship between advanced manufacturing processes, metallurgical microstructures, and the associated material properties of functional and structural alloys.

OLIVER DAVIS received the B.Eng. degree in materials engineering from the University of Loughborough, U.K., in 2017. After completing a year in industry at SG Technologies Ltd., Rainham, U.K., he re-joined the company, in 2017, and is currently the Product Development Manager. At SG Technologies, he has been involved heavily in working on soft magnetic materials, such as cobalt iron and soft magnetic composite materials for power train and electrical drive applications. He works on projects, where he aims to transfer research and development work into manufactureable processes for tier 1 automotive companies. He has experience of managing collaborative projects involving academic and industrial partners.

JOHN TAYLOR graduated in physics. He joined the Lucas Research Centre to study advanced applications for magnetic materials. In these years, there were major investigations into what then were novel NdFeB magnets and advanced research was possible with the many collaborative projects then supported by EU. He has developed a comprehensive DC/AC magnetic characterization laboratory in support of the wider Lucas Group and for some years, he was an Active Member of the IEC TC68 Committee. In 1997, he joined SG Technologies as a Product Development Manager and changed the product group to include soft magnetic materials and assemblies. In 2012, he became the Chairperson of SG Technologies Group having led a buyout of the company. He is still the active Research and Development and Managing Director. In his time, he has been a member of the Institute of Physics Magnetism Group Committee, was a Founder and later the Chairperson of the U.K. Magnetics Society, and has published and delivered many papers on the wider subject of the real properties of magnetic materials and their impact on the performance of electrical devices.

ALEXANDER M. KORSUNSKY received the Doctor of Philosophy (D.Phil.) degree from the Merton College, Oxford. He is currently a World-Leader in engineering microscopy of materials for optimization of design, durability, and performance. He leads the Multi-Beam Laboratory for Engineering Microscopy (MBLEM) at Oxford and the Centre for In-Situ Processing Science (CIPS), Research Complex, Harwell. He consults Rolls-Royce plc on residual stress and structural integrity. He was a Junior Research Fellow at the Fitzwilliam College, Cambridge, and a Lecturer at Newcastle University, before returning to academic position at Oxford. Each year, he gives several keynote and plenary lectures at major international conferences. He developed extensive links that included visiting appointments in Italy (Roma Tre), France (ENSICAEN), and Singapore (NUS, NTU, A*Star). He has coauthored books on fracture mechanics (Springer) and elasticity (CUP) residual stress (Elsevier). He has published 450 papers in scholarly periodicals on subjects ranging from multimodal 'live' microscopy, neutron and synchrotron X-ray analysis, contact mechanics and structural integrity to micro-cantilever biosensors, and size effects. He is a fellow of the Institute of Physics, London, U.K. He is a member of editorial boards of the *Journal of Strain Analysis for Engineering Design*, *FFEMS*, *TAML*, and the Editor-in-Chief of *Materials and Design*, a major interdisciplinary Elsevier journal (2021 impact factor 7.991).